

D3.3 Optimized on-board measurement system including PN2.5 sensor



Deliverable No.	3.3	
Deliverable title	Optimized on-board measurement system including PN2.5 sensor	
Deliverable type	Report	
Dissemination level	Public	
Deliverable leader	Graz University of Technology	
Contractual due date	31.08.2024	
Actual submission date	06.11.2024	
Version	1.0	
Written by	Helmut Krasa (TU Graz), Martin Kupper (TU Graz)	18.10.2024
Reviewed by	L. Ntziachristos (EMISIA), P. Dégeilh (IFPEN)	28.10.2024
Approved by	Partners validating	01.11.2024

Disclaimer

Funded by the European Union. Views and opinions expressed are however those of the author(s) only and do not necessarily reflect those of the European Commission or CINEA. Neither the European Commission nor CINEA can be held responsible for them.

Revisions table

Version	Date	Change
1.0	06.11.2024	First submission



Contents

Revisions table	1
Executive summary	3
List of abbreviations	3
List of figures	4
List of tables	4
1. On-Board Measurements on Category-L Vehicles.....	5
1.1 State-of-the-Art	5
1.1.1 State-of-the-Art PEMS and SEMS Devices	6
1.1.2 Effort within the LENS Project	7
2. Sensor for Particle Number Emissions of Category-L Vehicles Down to 2.5 nm...8	8
2.1 The LENS PN 2.5 nm Sensor Approach	8
2.2 Description of the PN 2.5 nm Sensor	9
2.2.1 Basics of condensation for particle counting	9
2.2.2 Basics of diffusion charging	10
2.3 Theoretical Modelling	10
2.4 Working Fluid determination	11
2.5 Experimental validation of the sensor concept	13
2.5.1 Experimental setup	13
2.5.2 Diffusion charger evaluation	14
2.5.3 Droplet size evaluation	15
2.5.4 Laboratory evaluation of the combined approach	15
2.6 Sensor verification with exhaust particles	18
2.7 Conclusion and outlook	19
References	20



Executive summary

This report presents the development and validation of new measurement system capable of detecting particle emissions as small as 2.5 nm in diameter. The sensor, developed as part of the LENS project, addresses critical challenges in measuring ultra-fine particles in real-world driving conditions. The system combines methods from particle counting (CPC) technology and diffusion charging methods, offering significant improvements in the limit of high particle number concentration compared to conventional CPCs. The developed sensor uses a condensation growth stage followed by an electrical detection method, allowing for the reliable detection of particles down to 2.5 nm. The primary challenge addressed is the limitation of existing commercial sensors, which either struggle to detect such small particles or require large and complex dilution systems, making them unsuitable for portable, on-road applications. The work contains theoretical modeling, laboratory testing, and on-road evaluations. Initial tests using Diethylene Glycol (DEG) as a working fluid have shown promising results, with the system detecting particle concentrations up to $1.5 \times 10^6 \text{ \#/cm}^3$. In conclusion, this report outlines a step forward in ultra-fine particle measurement. Further developments are planned to improve sensor performance for real-world applications, including optimizing the working fluid and improving the response time and accuracy.

List of abbreviations

LV	Category-L Vehicle
PEMS	Portable Emission Measurement System
SEMS	Smart Emission Measurement System
CPC	Condensation Particle Counter
RDE	Real Driving Emissions
PTI	Periodical Technical Inspections
PN	Particle Number
DEG	Diethylene Glycol
DC	Diffusion Charger
CVS	Constant Volume Sampling
CDC	Condensation Diffusion Charger
GMD	Geometric Mean Diameter



List of figures

Figure 1: Schematic representation of all components involved in a PEMS-setup.	5
Figure 2: Schematic representation of the PN 2.4 nm sensor. DC... diffusion charger, FCEM... Faraday Cup Electro Meter	9
Figure 3: Exemplary simulation results of the temperature- (left) and vapor saturation-profile (right) for a 2D- axial-symmetric tube. The center line is on the left side. Workingfluid: Diethylene glycol.....	11
Figure 4: Simulation of the critical size for particle activation (left) and the fraction of activated particle dependent on the initial particle size (center) and droplet size evolution for a 3.5 nm particle for three radial positions (right) Workingfluid: Diethylene glycol	13
Figure 5: Prototype characterization setup of the combined approach. The particles are generated by sublimation of solid NaCl in the tube furnace. After size selection through the classifier, the aerosol is split to the PN 2.5 nm sensor (growth chamber + Corona Charger & FCEM) and the reference CPC with additional dilution. The original concentration can be monitored directly by the reference instrument.....	14
Figure 6: Diffusion Charger characterization	14
Figure 7: Droplet size verification setup (left) and experimental results (right). The temperature in the legend indicated the difference between saturator and condenser. The condenser was kept at 20 °C.	15
Figure 8: Glycerol PN linearity test for two particle sizes	16
Figure 9: Particle activation test at two temperature differences with Diethylene Glycol. The PN concentration was at about 5000 cm ⁻³ for all particle sizes.....	17
Figure 10: Polydisperse measurement test with DEG as working fluid (temperatures 55°C and 20 °C)	17
Figure 11: Experimental measurement setup at the CVS at the LV chassis dyno at TU Graz.....	18
Figure 12: PN concentration comparison of CDC system with a reference sampling system. Concentrations are that of the CVS tunnel. The CDC signal: a) RAW, b) Experimental Correlation and c) best fit peak correlation. The CDC was limited to 106 #/cm ³ due to the calibration of the detector, the time resolution allows to capture the peaks.....	19

List of tables

Table 1: Overview about all portable measurement systems available in LENS, with analytes which can be measured.	6
Table 2: Working fluid parameters, at standard conditions.	12



1. On-Board Measurements on Category-L Vehicles

An overview about the current possibilities for the on-board measurement of emissions of category-L vehicles (LVs) was given in D3.1, here follows a brief summary.

1.1 State-of-the-Art

In general, two different kinds of measurement systems for the purpose of on-road emission measurement can be differentiated: i) Portable Emission Measurement Systems (PEMS) and ii) Smart Emission Measurement Systems (SEMS). The major differentiation is, that the first are systems consisting of exhaust flow measurement, sample dilution and preconditioning and high-accuracy analyser units, while the second are smaller and simpler systems, without sample conditioning and robust sensors. PEMS thus also require a more extensive preparation for mounting, need more power, thus a heavy battery pack, and are in total heavier. The increased weight might influence the emissions for light LVs, if mounting is possible at all. Despite all difficulties, PEMS allow to measure all analytes of interest at high accuracy, including particle number (PN) down to sizes of 10 nm. An exemplary overview of a PEMS system is given in Figure 1.

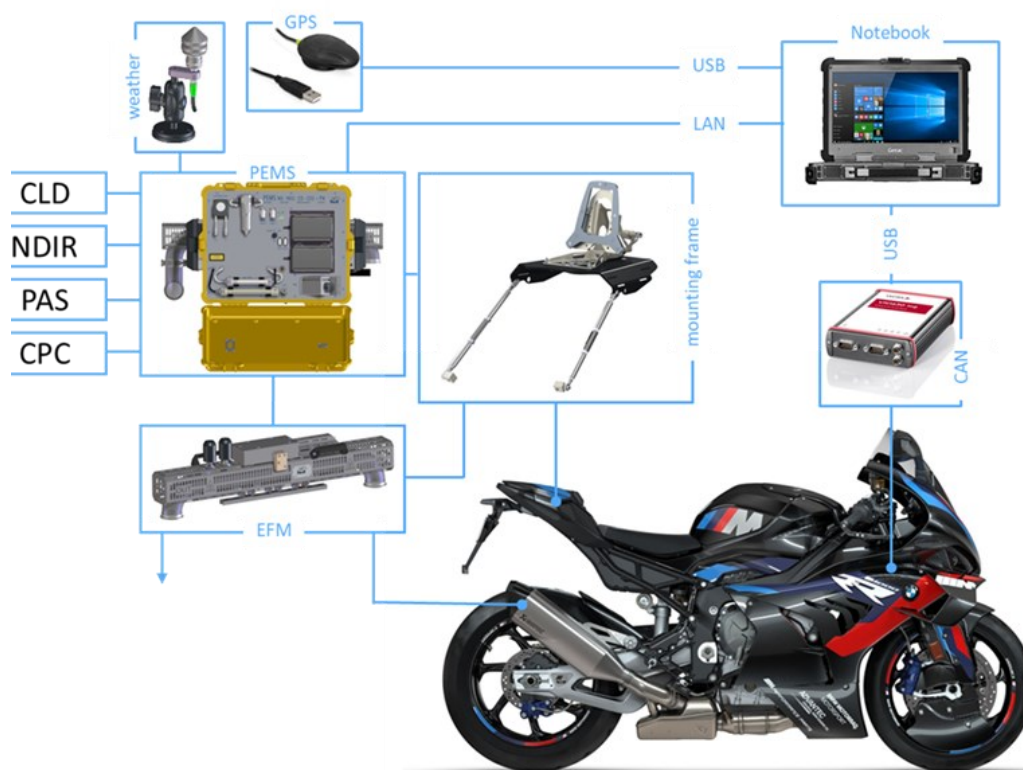


Figure 1: Schematic representation of all components involved in a PEMS-setup.

SEMS are smaller, lighter, are easier in application and require less power than PEMS, but the measurement accuracy is comparably poor and information about the exhaust mass flow cannot be obtained. Current limitations of SEMS measurements are also given by the sensor technologies, as the requirements for an easy application presuppose a robust sensor design, applicable on almost raw exhaust. As this was possible until now for gaseous analytes, reliable PN measurement for ultrafine particles (>100 nm) require a PEMS sample preconditioning.

1.1.1 State-of-the-Art PEMS and SEMS Devices

As described in D3.1 in detail the following PEMS and SEMS devices are available in the LENS consortium: AIP PEMS, HORIBA PEMS and SEMS, EMISIA ReTEMS, IFPEN REAL-e SEMS and CZU FTIR. These devices represent the State-of-the-Art of compact and beyond of portable emission measurement devices. Three of them can be equipped with particle sensors, of which the AIP PEMS uses a compact commercial CPC, the EMISIA ReTEMS uses a custom made QEPAS-sensor for black carbon measurement and the IFPEN REAL-e SEMS uses a diffusion charger, originally designed for PTI purposes.

Table 1: Overview about all portable measurement systems available in LENS, with analytes which can be measured.

AIP PEMS	HORIBA SEMS	HORIBA PEMS	EMISIA ReTEMS	IFPEN REAL-e SEMS	CZU miniPEMS
<ul style="list-style-type: none"> • CO • CO₂ • NO • NO₂ • (PN) 	<ul style="list-style-type: none"> • NO_x 	<ul style="list-style-type: none"> • CO • CO₂ • NO • THC (n-hexane equivalent) 	<ul style="list-style-type: none"> • CO • NO • CO₂ • PM (Black Carbon) 	<ul style="list-style-type: none"> • CO₂ • HC • CO • NO_x • NO • NO₂ • NH₃ • PN 	<ul style="list-style-type: none"> • CO • CO₂ • CH₄ • HCHO • NO • NO₂ • NH₃ • N₂O

The available particle sensors are fully functional within the possibilities of the sensor principle in the compact design. Only the ReTEMS sensor was custom made for the application and measures PM, which is relevant for particle sizes to 100 nm, smaller particles, even at high number concentration, do not contribute significantly to PM. The CPC in the AIP PEMS was designed for automotive applications, where detection limits at 23 and 10 nm are relevant and PN concentrations are comparably low to LVs, due to mandatory exhaust aftertreatment systems. The REAL-e SEMS uses an *Pegasor* PPSG2 which was actually developed for test-bench measurements. It is compliant to the PTI-sensor regulation and not specifically designed for measurements in idle. Although the measurement range is appropriate for LVs, the sensor signal of diffusion chargers shows a strong dependency to the particle size, overestimating large particles, while misprizing smaller ones, see section 3.2 for details. Furthermore, diffusion chargers are limited in the smallest detectable size by the size dependent charging efficiency, as described later in the report.



1.1.2 Effort within the LENS Project

In the LENS project we aim to characterise the PN emissions of LVs down to 2.5 nm in the lab and on-road. While this is possible in the lab, although very challenging, with state-of-the-art equipment, it is not known to the author that any portable sensor was ever realised. As it is important for a complete picture of LV emissions to compare the real driving emissions to measurements on a chassis dyno, it was decided in the project conception phase to develop a sensor prototype for the measurement PN to 2.5 nm.

This report focuses on the PN 2.5 nm sensor, multiple efforts were devoted to on-road emissions measurements by multiple LENS partners: Development and optimization of PEMS and SEMS, development of exhaust gas flow measurement approaches and the development of a miniaturized, high-resolution FTIR analyzer.



2. Sensor for Particle Number Emissions of Category-L Vehicles Down to 2.5 nm

2.1 The LENS PN 2.5 nm Sensor Approach

The PN sensor developed within LENS aims to detect particles down to 2.5 nm at high concentrations, while still being portable for on-road tests. The sensor approach combines electrical detection of aerosol with prior condensational growth. As stated in the previous chapter, currently such systems are commercially not available and also the existence of experimental devices is not known to the project members.

While condensation particle counters (CPCs) can directly count particles via light scattering and have the ability to detect particles below 3 nm, the upper concentration is limited by the optical counting as from a certain concentration on, particles overlap when passing the optics, causing so called “coinciding counts”. The single count regime is typically specified to concentrations below 30 000 #/cm³, above coincidence corrections must be applied. In exhaust PN concentrations of 10¹⁰ #/cm³ can be reached [1]. Considering the aforementioned limitations, a dilution ratio of roughly 1:30 000 would be required in order to be able to measure such high concentrations. This would demand very high flowrates within the dilution system, thus requiring high energy consumption and big pumps, not allowing for on-road measurements.

Measurement of particle concentration via electrical detection allows for detection of very high particle concentrations. Particle number counters for periodical technical inspections (PTI) based on diffusion charging (DC) can handle concentrations above 10⁶ #/cm³ without prior dilution [2]. However, DCs also do have certain drawbacks due to its indirect measurement approach of measuring the charge accumulating on the particles. Firstly, the measurement principle depends on the charging efficiency of particles, which is size dependent, thus the sensor signal is dependent on the particle size. Second, they are not capable of measuring particles in the single nm-size range, because of the very low charging probability. While certain methods can be used to reduce the size dependency, the fact that the DCs do actually not depend directly on the PN concentration cannot be neglected.

To overcome upper PN limit of CPCs while be able to measure down to the single digit nm regime with no influence of the particle size, we propose a PN sensor combining CPC and DC. In this approach particles are magnified in condensational growth stage and then high particle concentrations can be detected by diffusion charging. Particles above an adjustable size threshold grow into droplets of uniform size. Therefore, not the initial exhaust particles are measured, but the uniformly grown droplets. While the droplet size is a function of particle concentration, and therefore the sensor requires prior calibration, the particle size dependency is removed and therefore allows for measurement of PN concentration. This allows for i) detection of particles that were too small to be detected by diffusion charging directly, ii) removal of the inherent size dependency of diffusion charging-based methods and iii) increase the maximum measurable concentration drastically, compared to the single count regime of CPCs.



2.2 Description of the PN 2.5 nm Sensor

The sensor consists of a heated saturation stage, followed by a cooled droplet condenser stage, a charging stage and a faraday cup electrometer for signal detection. The test aerosol is saturated with a working fluid of choice at high temperature in the saturation stage. In the condenser stage, the aerosol with the saturated vapor is cooled down, causing a supersaturation of the working fluid vapor and subsequent condensational growth of the particles. Relevant details are described below. To obtain optimal working parameters and dimensions for construction of the condenser stage we run simulations, described in section 4. This allowed us to design the minimum detectable particle size as well as the droplet size, and thus the signal amplitude of the electrical detection.

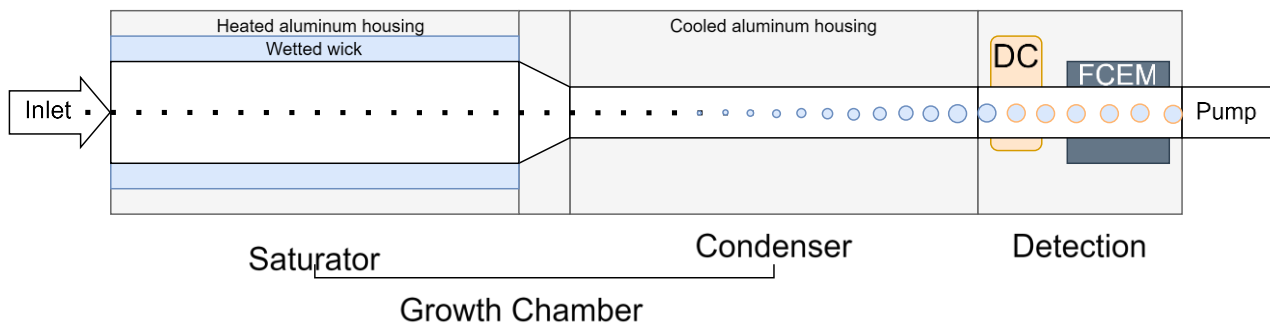


Figure 2: Schematic representation of the PN 2.4 nm sensor. DC... diffusion charger, FCEM... Faraday Cup Electro Meter

The diffusion charger uses a high-voltage corona to create ions. The ions are then guided towards the gas flow by an external electric field and attach on the aerosol particles driven by diffusional motion. The flow then passes an (optional) precipitator stage and finally enters the Faraday cup electrometer for signal detection. A more detailed description can be found below.

2.2.1 Basics of condensation for particle counting

In a CPC, particles are functioning as condensational seeds and then grown to a detectable droplet size through vapor condensation. By this approach it is possible to detect ultrafine particles, too small to be detected directly. Key is the exposure of particles to supersaturated vapor, which occurs when the vapor pressure exceeds the equilibrium vapor pressure. The thermodynamic drive towards the equilibrium vapor pressure is the reason for condensation. This can be described using the Kelvin equation [1]:

$$d_p = \frac{4 \sigma v_m}{RT \ln(S)} [1]$$

with Temperature T , gas constant R , surface tension σ , molar volume v_m , particle diameter d_p , and the supersaturation S , which is defined as the ratio of current vapor pressure to the saturation vapor pressure. From this equation follows that S must be higher, the smaller the d_p , to be able to activate the particle as a condensational seed for droplet growth. The curved particle surface raises the equilibrium vapor pressure. The supersaturation is. But evidently also material parameters of the working fluid are influencing this process. Influences from the seed particle are not considered by this theory. This activated particle size d_p , also known as the Kelvin-Diameter defines the lower size detection limit of the sensor in use.



2.2.2 Basics of diffusion charging

DCs for particle measurements operate by charging aerosol particles through the attachment of ions. In these devices, an aerosol has to be brought in contact with ions by mixture with an ion carrying gas or on-spot generation of ions, as e.g. by a corona discharge. As particles travel through this ion-rich environment, they acquire electrical charges, primarily through the diffusion of ions onto the particle surfaces. The amount of charge a particle acquires is dependent on the particle size. The charged particles are directed to an electrometer for detection, where the total charge is measured. The variation of the corona current, the introduction of a precipitation stage between the corona charger and the detector, or the introduction of a second detector stage, allows for an estimation of the average particle size distribution, if needed.

However, due to its indirect measurement principle, the signal correlates strongly with particle size, not allowing for a direct measurement of the PN concentration. For DCs, this typically scales with $\sim d^x$ with the scaling factor x being in the region of 1.1 to 1.2, so therefore scaling is close to linear with particle size [3]. Therefore, instead of the total particle number, the total particle length is measured. Furthermore, the charging efficiency for particles below 30 nm tends to drop off sharply, due to the inability of small particles to carry even single charges, or in other words, to be attached to ions [4]. Thus it is favorable for DC sensors if the measured particles are not too small and ideally all of the same size, as it is the case in the proposed concept.

2.3 Theoretical Modelling

To calculate the minimum detectable particle size (i.e. the Kelvin-Diameter), the supersaturation of the working fluid vapor in the saturator is needed, and connected with this also the temperature und vapor concentration distribution. We set up a 2D-axisymmetric COMSOL model which solves for fluid flow to obtain the flow field, heat transfer for the temperature distribution and the diffusion-convection equation for the vapor distribution. Input variables were the flow rate Q , temperatures of the saturator (hot section) and condenser (cold section), as well as geometric factors of the growth stages: tube diameter, and the lengths of saturator, condenser and the insulator in-between. The flow rate in combination with the surface-to-volume ratio defines the required lengths to i) fully saturate the gas with the working fluid and ii) allow for sufficient time of particle growth. The particle growth was then modeled to get an estimate of the droplet size. An example of a temperature- and vapor-field is shown in Figure 3. The initial parameters were chosen to be similar to that of a conventional CPC to allow for comparison of the demonstrator.



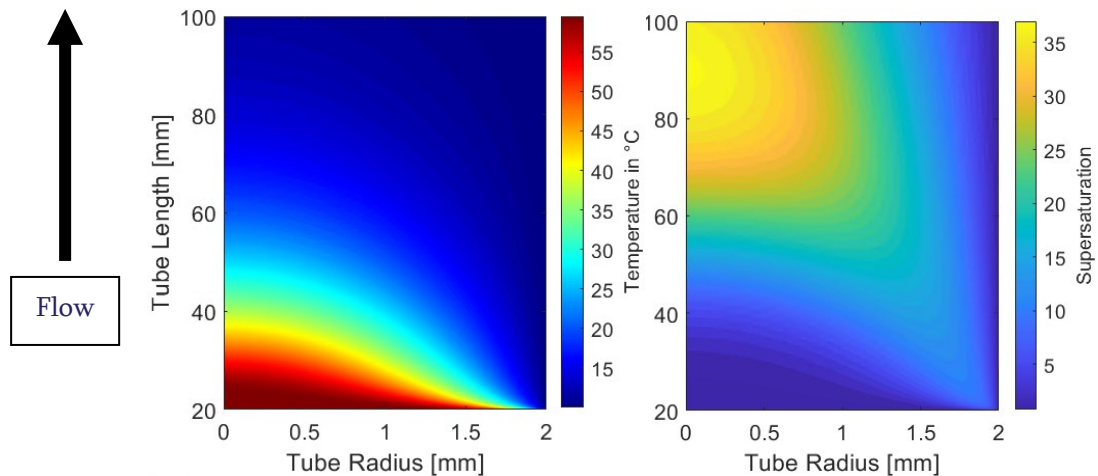


Figure 3: Exemplary simulation results of the temperature- (left) and vapor saturation-profile (right) for a 2D-axial-symmetric tube. The center line is on the left side. Workingfluid: Diethylene glycol

2.4 Working Fluid determination

A careful selection of an appropriate working fluid is of great importance for the adaptation of condensation particle magnification technology to certain applications. Due to the wide possibilities of working fluids substances at a first glance, we defined key parameters to refine the selection. The most common working fluid in conventional CPCs is n-Butanol and was considered first. It was excluded as homogeneous nucleation starts at the high supersaturations, which are required to active 2.5 nm seeds. Homogeneous nucleation means that the own molecules of the working fluid substance trigger droplet growth even without seed particles present. Furthermore, droplets would grow into sizes $> 10 \mu\text{m}$ from the required supersaturation, which are then very prone to losses due to gravitational settling and inertial effects. Larger droplets are also prone to changes in size at PN high concentrations, as the vapor uptake by these droplets is high enough to cause depletion effects within the growth chamber, leading to reduced supersaturation profiles and therefore smaller droplet diameters, which then again directly influence the sensor signal. However, this effect can be measured empirically and be corrected for. This illustrates that the selection criteria for working fluids to magnify particles below 4 nm differ from that of a conventional CPC.

The problem of working fluid selection is multi-faceted and was done by a systematic approach. Some limit values were found obvious, such as the melting and boiling point, as the fluid should be in liquid state in the useable temperature range. To balance the influences of surface tension and vapor pressure requires very careful considerations, as both heavily influence the homogenous nucleation limit, final droplet size and wettability of the wick. In Table 2 the considered parameters and are listed with defined threshold values, if possible. A material database was used to scale down the number of working fluids. A list of currently 70 working fluids is currently being evaluated. Parameters outside of this table, which could not be filtered for, are acute toxicity, pricing, availability of the fluid of choice, wettability with wick material as well as their growth behavior on different particle seed materials. Based on this criteria, one to two suitable working fluids are planned to be tested with the next instrument generation.

Table 2: Working fluid parameters, at standard conditions.

Material parameter	Limit	Relevance
Melting point	< 20 °C	Liquid state
Boiling point	> 60 °C	Liquid state
Flame point	> 60 °C	Safety concern
Vapor Pressure	< 5e-3 mmHg	Droplet size, hom. Nucl. limit
Surface Tension	10 σ < 130 dyne/cm	Wettability, hom. Nucl. limit
Diffusion Coefficient, rel. to thermal air diffusion coeff.	<0.8 or >1.2	Supersaturation generation
Toxicity	Low is better	Safety concern
Log-octanol-water solubility	Higher is better	Water retention, wick longevity
Polarity	Low is better	Influence on particle growth
Viscosity	Low is better	Wick wettability

Diethylene Glycol (DEG) was found to be a suitable working fluid, as it is already in use particle size magnifiers or sub-2 nm CPC boosters. Due to the low vapor pressure the droplets do not grow large enough to be detected directly by light scattering. For the booster stages, it is sufficient, that the DEG CPCs enhances the particle size to be comfortably in the plateau region of a CPC, which starts typically somewhere between 10 and 50 nm. However, the droplet sizes from DEG particle magnifiers can also be detected by electric particle sensors (Figure 4, right). A downside of DEG is the high-water affinity, which causes the wick to take up water and thus reduces the vapor pressure, causing a long-term drift.

All particles that do trigger droplet growth do cause a sensor signal in the end. In the design of such a sensor the lower limit of droplet growth one has to take care to obtain similar sized droplets, independent of the initial particle size. Other considered working fluids such as, e.g., Glycerol, have very low vapor pressure. For Glycerol droplets only grow to a few hundred nm, and as seed particles might be in this size regime the droplet size is not independent of the initial particle size. Another important effect is the effective time of droplet growth. As shown in Figure 4, left, smaller particles tend to activate later in the condenser, meaning that there is a shorter growth time to grow available, causing a disparity between small and large particle seeds, which compensates more if the droplets grow large compared to the seed size. Above 500 nm in droplet size, the size dependency of the droplet on the initial particle becomes negligible. The final droplet size is dependent on the supersaturation, temperature and residence time in the condenser. Droplets passing the center region are slightly larger than those close to the walls, due to the supersaturation distribution. The parabolic flow profile however, increases the residence time of particles further away from the center line (see the increased growth time in the right of Figure 4) and thus partially compensating the effect caused by reduced supersaturation closer to the walls. A slight manipulation of the estimated droplet size can be performed by changing the whole temperature range, while keeping the temperature difference between saturator and condenser constant. I.e., if both the temperatures of the saturator and condenser are reduced by 10 °C, the saturation profile remains largely constant, keeping the activated particle sizes almost the same (within 2% of the nominal size), while the estimated droplet size in Figure 4 reduced from 1.14 μm down to 0.69 μm .



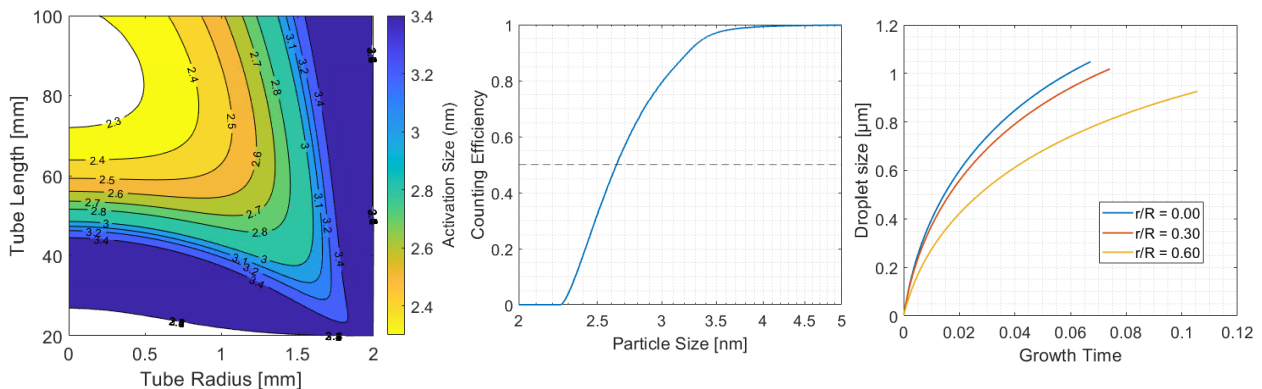


Figure 4: Simulation of the critical size for particle activation (left) and the fraction of activated particle dependent on the initial particle size (center) and droplet size evolution for a 3.5 nm particle for three radial positions (right) Workingfluid: Diethylene glycol

2.5 Experimental validation of the sensor concept

2.5.1 Experimental setup

A demonstrator of the sensor concept was evaluated in the lab to verify the simulations and find a setup to achieve the target specifications. The performance was evaluated in the lab in comparison to reference instruments using a lab generated model aerosol. The growth chamber was realized basing on the simulations and tested on its own as well in combination with the diffusion charger.

The experimental setup is shown in Figure 5. For all measurements an aerosol from NaCl particles was used, generated by the evaporation-condensation method according to Scheibel and Porstendörfer [5]. A small ceramic boat containing NaCl was placed inside the quartz tube in the center of the Carbolite MTF 12/38/250 tube furnace and heated up to 750 °C. Nitrogen was used as the carrier gas. After passing through the tube furnace, the gas was cooled down in a cooling spiral, causing supersaturation and subsequent nucleation of the salt vapor. For larger particle sizes, a dilution bridge was used to stay within the single count range of the CPC.

Particles were classified by their electrical mobility diameter using a TSI 3083 classifier and a TSI 3088 X-ray source. Depending on the particle size, either a TSI 3081 long DMA for larger particles or a 3086 nano DMA for smaller particles was used. The sheath-to-sample flow rate was set to > 10:1 to ensure highly monodisperse aerosol after size selection.

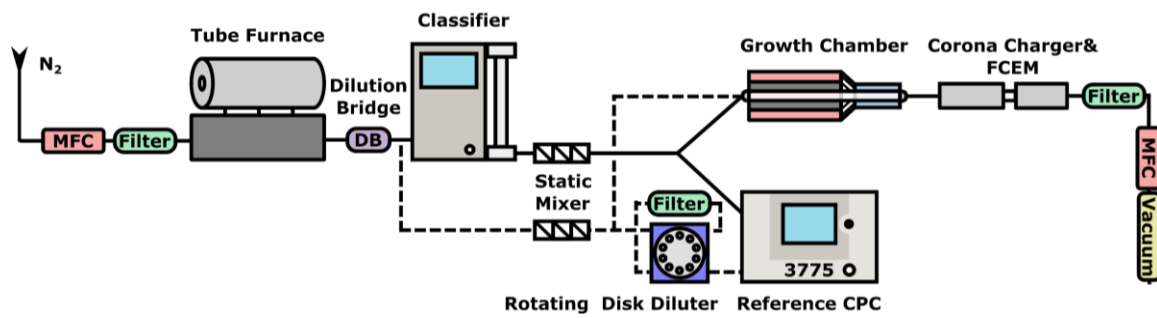


Figure 5: Prototype characterization setup of the combined approach. The particles are generated by sublimation of solid NaCl in the tube furnace. After size selection through the classifier, the aerosol is split to the PN 2.5 nm sensor (growth chamber + Corona Charger & FCEM) and the reference CPC with additional dilution. The original concentration can be monitored directly by the reference instrument.

2.5.2 Diffusion charger evaluation

First the diffusion charger was evaluated without the growth chamber. Diffusion chargers are known for the wide linear range, so the focus of this test was on evaluation of the size-dependent counting efficiency (CE) of the diffusion charger. The setup in use is shown with solid lines in Figure 5, without the growth chamber. The sensor signal of the diffusion charger was found as expected, with an exponential signal increase of 1.18, being close to linear with particle size. Also, the calibration of the sensor was working as intended, with a variation of less than 2% of the set counting efficiency of 1 at 50 nm. Therefore, no additional calibration was performed.

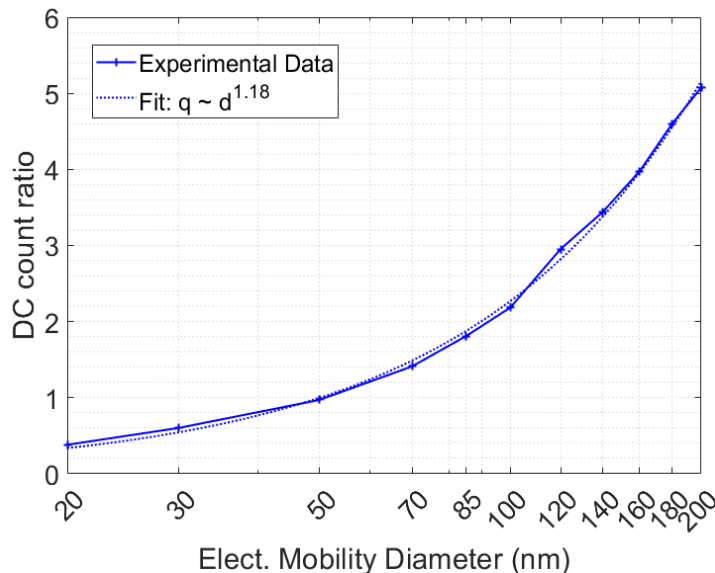


Figure 6: Diffusion Charger characterization



2.5.3 Droplet size evaluation

Second, the droplet size of the growth chamber was measured and compared with the simulation results. The droplet sizes were measured with a TSI APS. Since a flow of 5 l/min is required for the APS, additional particle free air was added to the system. The results show very good agreement with the simulation independent of the particle size, which was kept between 10 and 100 nm. At larger particle sizes and larger initial particle diameters, we have seen a slight reduction in droplet size.

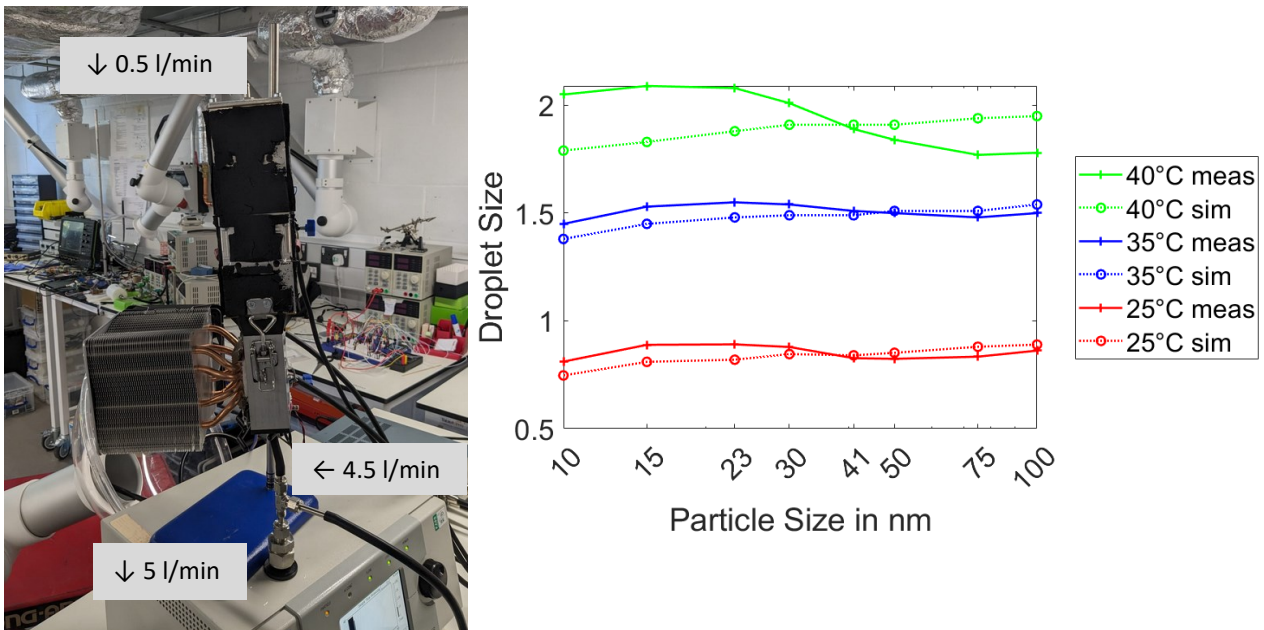


Figure 7: Droplet size verification setup (left) and experimental results (right). The temperature in the legend indicated the difference between saturator and condenser. The condenser was kept at 20 °C.

Due to larger PN concentrations of bigger particles sizes, vapor depletion effects slightly decreased the droplet size, this effect was therefore not one of initial particle size, but PN concentration. The effect was stronger for bigger droplets which take up more vapor (vapor mass uptake scales with r^3), at lower temperatures and smaller concentrations, this effect was not observed.

2.5.4 Laboratory evaluation of the combined approach

After showing that the growth stage and the diffusion charger work as intended, the performance of the whole sensor concept - condensation diffusion charging (CDC) - was evaluated with the setup shown in Figure 5.

First performance tests were performed with Glycerol as a working fluid. A PN linearity test was performed, the experimental results are shown in Figure 8. With Glycerol having a lower vapor pressure, droplets have been expected not grow as large as with DEG. At low concentrations the sensor amplification was between 5.7 and 6 for a temperature setting of 60 °C for the condenser and 20 °C for the saturator. This agrees well with theoretical size calculations. With the signal amplification of $d^{1.18}$, and a signal strength of 1 at $d = 50$ nm, the estimated experimental droplet size is 228 nm. This agrees within 5 % of the simulated droplet size of 244 nm. At lower temperature differences, the simulation was underestimating the droplet size by up to 30 %. Glycerol however, showed reduced counting performance after repeated measurements. This was

most likely caused by water uptake from the wick and causing a decrease in vapor pressure and therefore a reduction in sensor signal. PN concentrations up to $2 \cdot 10^6 \text{ cm}^{-3}$ were measured.

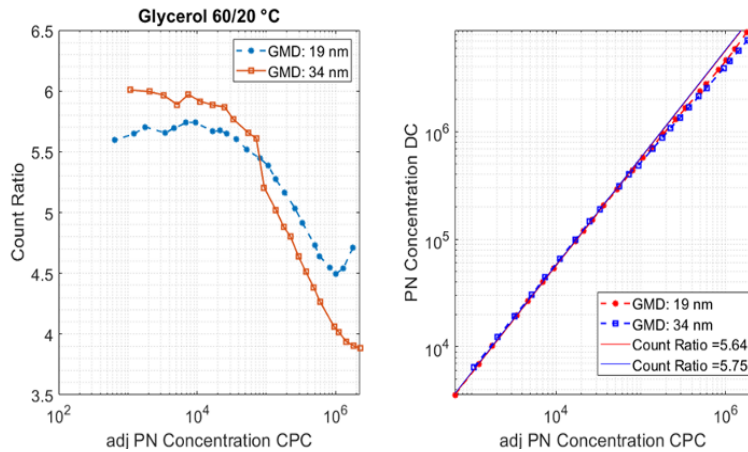


Figure 8: Glycerol PN linearity test for two particle sizes

Compared to Glycerol, DEG behaved as expected according to the simulation. Due to the higher vapor pressure, the droplet size is bigger, leading to a stronger signal amplification. Furthermore, vapor depletion effects can be observed at lower PN concentrations. In order to avoid homogenous nucleation of DEG vapor, the temperature difference between condenser and saturator was lowered by 5 °C to 55 °C for the saturator and 20 °C for the condenser. Furthermore, at a lowered temperature setting (40°C saturator temperature), the efficiency evaluation was tested as well.

The TSI 3775 CPC has a specified detection limit at 4 nm, thus we used an aerosol electrometer as reference instrument for these measurements. The particle concentration was kept at about 5000 \#/cm^3 . The resulting data is shown in Figure 9. The overall measured activation curve agrees very well with that of the simulation and shows that particle activation down to 2.5 nm is feasible with the setup in use. The influence of the chemical interaction of working fluid and particle seed material, which can cause a shift over 50 % in counted particle size (as e.g shown in [6]) for 23 nm CPCs might also be of interest here, although the effect is known to decrease with rising supersaturation [7].

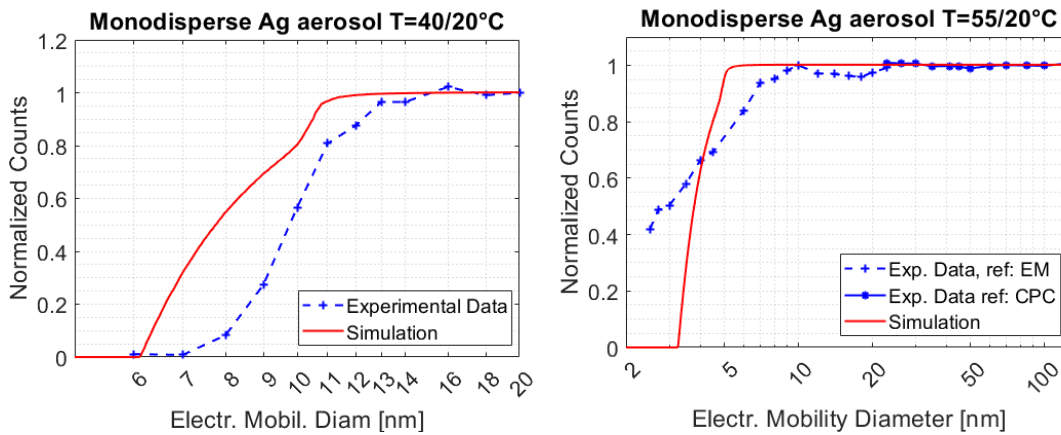


Figure 9: Particle activation test at two temperature differences with Diethylene Glycol. The PN concentration was at about 5000 cm^{-3} for all particle sizes.

Similar to Figure 8, the linearity was evaluated with DEG as a working fluid. Since the goal of detecting 2.5 nm aerosol was achieved using a temperature setting of 55/20 °C for the saturator and condenser, those were the settings used for all further measurements, including that with the CVS tunnel. The calibration factor was then used for the polydisperse measurement in Figure 10. The counting amplitude with regard to the PN concentration is shown. Due to vapor depletion (reduction of vapor due to uptake by the particles) and condensational heating (caused by the latent heat of the vapor), the vapor concentration is reduced and the temperature slightly increased, causing the droplet growth to reduce. The absolute signal amplification is about a factor of 10 higher, therefore leading to a signal amplification of 10 at low concentrations and 5 at high concentrations. This leads to a signal decrease of about 50 % at $1.5 \cdot 10^6$ compared to low concentrations, which gives a raw sensor signal for $7.5 \cdot 10^6$. This decrease in signal however is dependent on the PN concentration only and not the particle size. Thus it can be calibrated for, similar to that of the coincidence correction of a CPC.

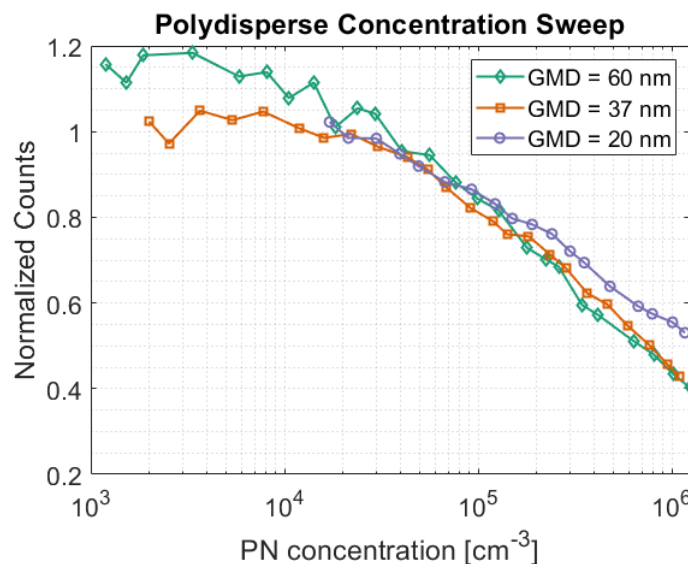


Figure 10: Polydisperse measurement test with DEG as working fluid (temperatures 55°C and 20 °C)



2.6 Sensor verification with exhaust particles

After evaluation of the sensor signal in the laboratory, the sensor was put into test on a LV chassis dynamo at Graz University of Technology. Due to the current sensor limit of about $1.5 \cdot 10^6 \text{ \#/cm}^3$ without any dilution system, the sensor was put into the CVS tunnel and sampled parallel to the TUG sampling system, which uses a CPC with a prior 1:260 air dilution and a PCRF of 1:517. The sampling system can be seen on the left side of Figure 11, whereas the CDC sensor is shown on the right hand side on expanded polystyrene boxes. Due to initial limitations, the sensor was compared to a 10 nm CPC. Furthermore, this CPC reference system contains a catalytic stripper that removes semi-volatile particles, whereas the CDC sensor measures the total particle number down 2.5 nm.

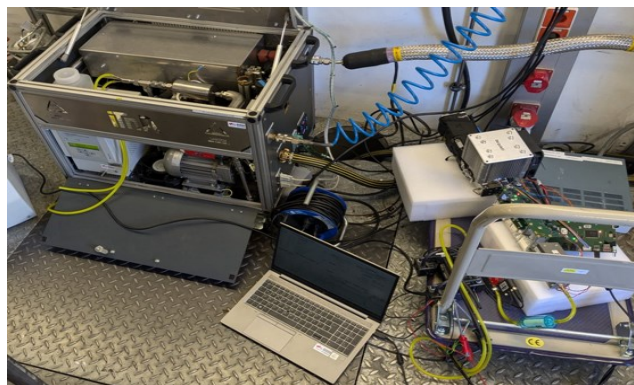


Figure 11: Experimental measurement setup at the CVS at the LV chassis dynamo at TU Graz.

The resulting raw-signal comparison is shown in the upper graph of Figure 12. The CDC signal overall overestimates in comparison the reference. This behavior was expected, as the DC was not adjusted for the comparably large droplets from the condensation chamber. The signal was corrected by concentration-dependent signal decrease as measured in Figure 10 and the result is shown Figure 12 in the middle graph. The maximum measured concentration in the raw data was limited in the DC to about $7 \cdot 10^6 \text{ \#/cm}^3$ by means of the original calibration, which is transferred to the current actual sensor limit of about $\sim 1 - 1.5 \cdot 10^6 \text{ \#/cm}^3$ in the actual size dependent calibration, as shown in Figure 12 in the lower graph.

In order to investigate the potential of the obtained data, we improved the correlation with the reference signal in a postprocessing step, by manually analyzing peak heights of both datasets, and fitting the data with a potency fit. The resulting data is shown in the lower graph of Figure 12. The data shows good correlation of the two PN emission data, however, the highest emission peak event between 11:40 and 11:45, cannot be accounted for, since the CDC signal saturated. In order to increase the measurable PN concentration, the analog-digital-converter of the diffusion charger is planned to be lowered to increase the maximum PN concentration. Furthermore, a dilution prior to the sensor will be put into place to increase the response time.

Besides the described CDC upper PN limit, further limitations within this evaluation lead to a decrease in signal correlation. First, the necessary pulsing of the DC, which decreases the response time to a maximum frequency of 1 Hz within the current setting. This can be decreased by increasing the flow through the DC sensor, however in turn, this would require higher flows for an eventual dilution system. Second, the response time was worsened by the long residence time ($\sim 3 \text{ s}$) of the connection between the CVS tunnel and the sensor caused by the low flow rate in use. This problem is caused by the limitations within this



experimental setup and not generally a limitation of the sensor concept. Third, the correlation between total PN at 2.5 nm and solid particles with a 10 nm CPC can be significant for most emission events, but differences can be expected as the measurands are actually different. Measurements in comparisons with a 2.5 nm CPC for total PN are scheduled within the project.

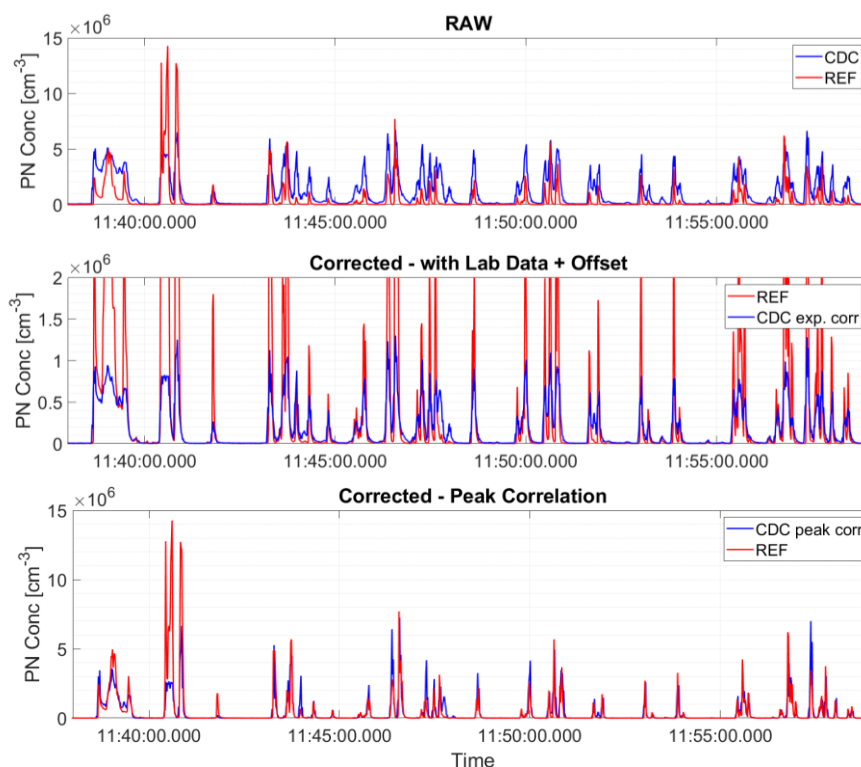


Figure 12: PN concentration comparison of CDC system with a reference sampling system. Concentrations are that of the CVS tunnel. The CDC signal: a) RAW, b) Experimental Correlation and c) best fit peak correlation. The CDC was limited to 10^6 #/cm³ due to the calibration of the detector, the time resolution allows to capture the peaks.

2.7 Conclusion and outlook

In conclusion, the development and testing of the PN 2.5 nm sensor have provided a promising approach for improving the RDE measurement of ultrafine particles in vehicle emissions. The sensor combines diffusion charging with a condensation growth stage, and enables the detection of particles as small as 2.5 nm and measurements at high concentrations.

Simulations indicate strong agreements concerning the minimum detectable particle size. Laboratory and measurements on exhaust indicate that the sensor performs as intended, however for the system to perform reliably for on-board measurements further improvements are required.

This includes aspects such as decreasing response time and improving calibration under varying particle concentrations, as adding a dilution unit and tuning the parameter of the DC system to increase the concentration limit further. Current progress shows that high PN concentration measurements are possible without requiring very high dilution ratios. Further work also includes the search for suitable alternatives regarding the working fluid as well as exploring the long-term stability of the sensor concept.



References

- [1] S. Schurl, M. Kupper, H. Krasa, A. Heidinger, and S. Schmidt, “A PN-Measurement System for Small Engine Applications,” 2023.
- [2] A. Melas, K. Vasilatou, R. Suarez-Bertoa, and B. Giechaskiel, “Laboratory measurements with solid particle number instruments designed for periodic technical inspection (PTI) of vehicles,” *Measurement*, vol. 215, p. 112839, Jun. 2023, doi: 10.1016/J.MEASUREMENT.2023.112839.
- [3] R. T. Nishida, N. M. Yamasaki, M. A. Schriefl, A. M. Boies, and S. Hochgreb, “Modelling the effect of aerosol polydispersity on unipolar charging and measurement in low-cost sensors,” *J Aerosol Sci*, vol. 130, pp. 10–21, Apr. 2019, doi: 10.1016/J.JAEROSCI.2019.01.003.
- [4] M. A. Schriefl, A. Bergmann, and M. Fierz, “Design principles for sensing particle number concentration and mean particle size with unipolar diffusion charging,” *IEEE Sens J*, vol. 19, no. 4, pp. 1392–1399, Feb. 2019, doi: 10.1109/JSEN.2018.2880278.
- [5] H. G. Scheibel and J. Porstendörfer, “Generation of monodisperse Ag- and NaCl-aerosols with particle diameters between 2 and 300 nm,” *J Aerosol Sci*, vol. 14, no. 2, pp. 113–126, 1983, doi: 10.1016/0021-8502(83)90035-6.
- [6] X. Wang, R. Caldow, G. J. Sem, N. Hama, and H. Sakurai, “Evaluation of a condensation particle counter for vehicle emission measurement: Experimental procedure and effects of calibration aerosol material,” *J Aerosol Sci*, vol. 41, no. 3, pp. 306–318, 2010, doi: 10.1016/J.JAEROSCI.2010.01.001.
- [7] Wlasits, P. J., Stolzenburg, D., Tauber, C., Brilke, S., Schmitt, S. H., Winkler, P. M., & Wimmer, D. (2020). Counting on chemistry: Laboratory evaluation of seed-material-dependent detection efficiencies of ultrafine condensation particle counters. *Atmospheric Measurement Techniques*, 13(7), 3787–3798. <https://doi.org/10.5194/amt-13-3787-2020>

